Molecular Crystals and Liquid Crystals
Publication details, including instructions for authors and subscription information:
http://www.tandfonline.com/loi/gmcl16

Studies of Band-Structure, Excitonic Processes and Trap Distribution in Pyrene

J. Gonzalez Basurto [a b] , Z. Burshtein [a] & J. Levinson [a c]
[a] The Racah Institute of Physics, The Hebrew University of Jerusalem, Israel
[b] Escuela de fisica, I.P.N., Mexico City, Mexico
[c] Soreq Nuclear Centre, Yavne, Israel
Version of record first published: 21 Mar 2007.

To cite this article: J. Gonzalez Basurto , Z. Burshtein & J. Levinson (1975): Studies of Band-Structure, Excitonic Processes and Trap Distribution in Pyrene, Molecular Crystals and Liquid Crystals, 31:1-2, 131-144

To link to this article: http://dx.doi.org/10.1080/15421407508082865

Mol. Cryst. Liq. Cryst., 1975, Vol. 31, pp. 131–144

Printed in Holland

Studies of Band-Structure, Excitonic Processes and Trap Distribution in Pyrene†

J. GONZALEZ BASURTO,‡ Z. BURSHTEIN and J. LEVINSON§

The Racah Institute of Physics, The Hebrew University of Jerusalem, Israel

(*Received April 7, 1975*)

Photocurrent measurements are used to study conduction-band structure, electron trap characteristics and optical de-trapping processes in pyrene crystals. The spectral yield of the photocurrent arising from photoexcitation of trapped electrons indicates the existance of a series of narrow ($\lesssim 0.1$ eV) conducting sub-bands which constitute the bottom of the conduction band. A broader band ($\gtrsim 0.25$ eV), about 0.45 eV above the lowest lying conduction sub-band, is also revealed. In the triplet range, de-trapping of electrons by photo-generated triplet excitons is found to be the dominant mechanism. The crystals under study were found to contain three sets of electron traps, each of density of about 5×10^{11} cm^{-3} located at about 1.35, 2.07 and 2.4 eV below the lowest conduction band. The cross sections for direct photoexcitation and for de-trapping of electrons by triplet excitons are 5×10^{-17} cm^2 and $\sim 10^{-15}$ cm^2 respectively for the first set, and 5×10^{-18} cm^2 and $\sim 10^{-16}$ cm^2 for the second set of traps.

INTRODUCTION

Measurements of photocurrents arising from optical excitation of trapped electrons[1] and holes[2] in anthracene were reported previously. Characterization of the traps (density, energy distribution and excitation cross-sections) provided valuable information on the conduction and valence band structure in anthracene.[1,2] In the present work, the methods used in these studies were extended to pyrene. As before, the photocurrents measured involved the excitation of trapped electrons injected into the sample by an ohmic contact (Hg–Na amalgam). Vapour-grown pyrene crystals were found to contain

† This work was carried out within the framework of the scientific joint program between the Mexican Council for Science and Technology and The Israel National Council for Research and Development.

‡ Permanent address: Escuela de fisica, I.P.N., Mexico City, Mexico.

§ Present address: Soreq Nuclear Centre, Yavne, Israel.

three main sets of traps, each of density of about 5×10^{11} cm^{-3}, located at about 1.3, 2.07 and $\sim$2.4 eV below the lowest conduction band. The two shallower sets are essentially discrete in energy, which is a valuable advantage in the study of the conduction band structure. The spectral response of the photocurrent yield in the low photon energy range (1.2–2.05 eV) is found to originate from de-trapping of electrons out of the shallow set by direct photoexcitation. The structure in this range indicates the existence of a series of narrow ($\leq$0.1 eV) conduction sub-bands. About 0.45 eV above the lowest-lying conduction sub-band, a broader band ($\gtrsim$0.25 eV) could also be identified. For shorter wavelengths (2.09 eV $< h\nu <$ 2.4 eV), photo de-trapping occurs mainly by interaction of photo-generated triplet excitons with the trapped electrons. In this range however, the *two* shallow sets of traps are involved. In the range $h\nu >$ 2.4 eV, an additional set participates but the origin of the photocurrents is not entirely clear. It can be due to direct photoexcitation and/or excitation through the interaction of photo-generated singlet excitons with the trapped electrons. The cross sections for direct photoexcitation and for de-trapping of electrons by triplet excitons for the two shallow sets were determined.

EXPERIMENTAL

The measurements were carried out on pyrene crystals grown by sublimation. The samples were thin platelets (50–100 μ in thickness), oriented parallel to the (a, b) plane, as directly obtained from the growth batch. The samples were enclosed in sandwich type cells, one electrode being a transparent conducting glass, the other an electron-injecting Na–Hg amalgam contact.[1] The sample holder, the current and photocurrent measuring circuit and the optical system were similar to those described previously.[1]

RESULTS AND DISCUSSION

Appreciable dark currents were observed only when the applied dc voltage was such as to make the Na–Hg amalgam electrode negative. This polarity is referred to as the "forward" polarity and corresponds to electron injection from the amalgam. As in the case of electron or hole injection into anthracene,[1,2] the injected electron space-charge-limited current can be enhanced by illumination. Also, *after* a forward voltage has been applied (in the dark), a photocurrent in the reverse polarity ("reverse photocurrent") is observed, a photocurrent that decays with time of illumination. The photocurrents in both forward and reverse polarities are associated with the photoexcitation

of electrons from traps, filled-up by injection. (In the case of the reverse photocurrents, the electron traps have been filled by prior application of the forward injecting voltage.) The method used for the characterization of the traps and its consequences is described in detail in references 1 and 2.

In Figure 1, the dark currents and the forward and reverse photocurrents are plotted on a log-log scale as functions of the *forward* (injecting) voltage. The photocurrents were obtained by illumination with light of wavelength $\lambda = 0.55\ \mu$ ($h\nu = 2.26$ eV) and of intensity 3.5×10^{14} photons/cm^2 sec.

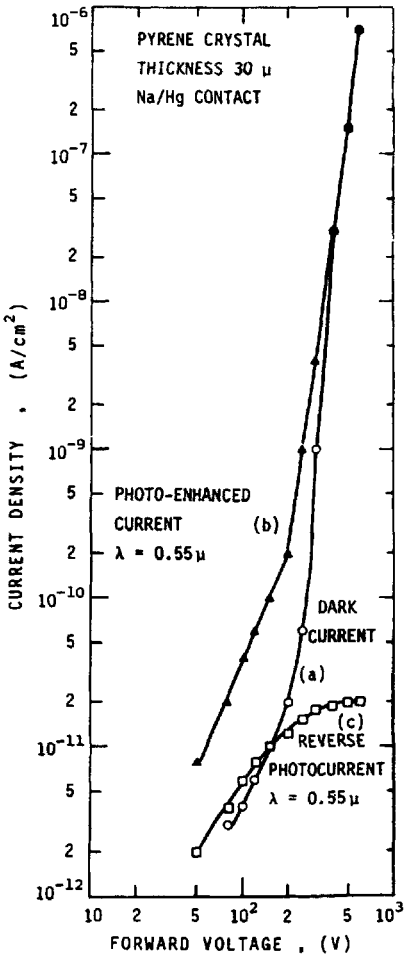

FIGURE 1 Log-log plots of dark (curve (a)), of photo-enhanced space-charge-limited current (curve (b)) and of saturated reverse photocurrents (curve (c)) as functions of injecting voltage. The light intensity ($\lambda = 0.55\ \mu$) if $F = 3.5 \times 10^{14}$ photons/cm^2 sec.

The forward photocurrents (curve (b)) are photo-enhanced space-charge-limited currents,[1,2] photoexcitation of electrons out of traps produced by the illumination acting to increase the ratio of free to trapped charge. The reverse photocurrent corresponding to a given *forward* voltage was obtained as follows. The forward voltage is first applied for a few minutes (in the dark) to allow for a fraction of the traps to be filled by the injected electrons. The voltage polarity is then reversed and the initial photocurrent following illumination is measured (the reverse voltage is made sufficiently large so as to prevent re-trapping of photoexcited electrons—see next Figure). The reverse photocurrent measured in this manner (curve (c)) is seen to saturate for an injecting voltage of about 400 V. This voltage represents the trap filled limit V_{TFL} for which the injected space-charge is sufficient to fill up all the available electron traps. About the same value for V_{TFL} is provided by the steep rise of the dark current with voltage (curve (a)) starting at about 200 V.[1,3] To within a factor of two or so, the density N_t of these traps is given by[3] $(2\kappa\varepsilon_0/qL^2)V_{TFL}$, where ε_0 is the permitivity of free space, κ the relative dielectric constant, q the electronic charge and L the sample's thickness. Using the values $\kappa = 4$, $I = 35\ \mu$ and $V_{TFL} = 400$ V one obtains $N_t \approx 5 \times 10^{13}\ cm^{-3}$. As will be shown later, only *part* of these traps is responsible for the observed reverse photocurrents.

The variation of the reverse photocurrent with reverse voltage is shown in Figure 2. The forward injecting voltage applied prior to the measurement had been 400 V. The curve is seen to start out linearly and to saturate at higher voltages. The voltage V_c, at which the transition from linear to saturation conditions occurs, is about 150 V. This means that at this voltage

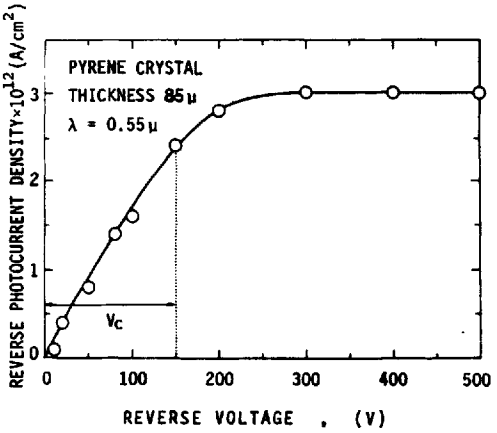

FIGURE 2 Reverse photocurrent as function of reverse voltage. Illumination conditions same as in Fig. 1. Forward injecting voltage applied prior to measurement was 400 V.

the electron schubweg $\mu_n(V_c/L)\tau_t$, where μ_n is the electron mobility and τ_t the electron trapping time, is comparable to the sample's thickness L. Using the value[4] of 0.5 $cm^2/V \cdot sec$ for μ_n, one obtains an estimate of ~ 1 μsec for the trapping time. The reverse photocurrent density shown in Figure 1 (curve (c)), as well as all other reverse-photocurrent measurements to be presented below correspond to the *saturated* photocurrent as obtained under a reverse voltage of 400 V.

The spectral response of the forward and reverse photocurrents is presented in Figure 3. Curve (a) is the spectral yield of the saturated photocurrent in the reverse non-injecting polarity, without prior injection in the forward polarity. This photocurrent does not involve injected electrons and is of no direct interest in the present investigation. Curve (b) is the spectral yield of the photo-enhanced space-charge-limited currents[1] obtained with a forward (injecting) voltage of 400 V. The photocurrents are between one to two orders of magnitude higher, revealing pronounced structure, which is lacking in curve (a). Almost an identical structure is seen in curve (c), which is the spectral yield of the saturated reverse photocurrents that follow a prior

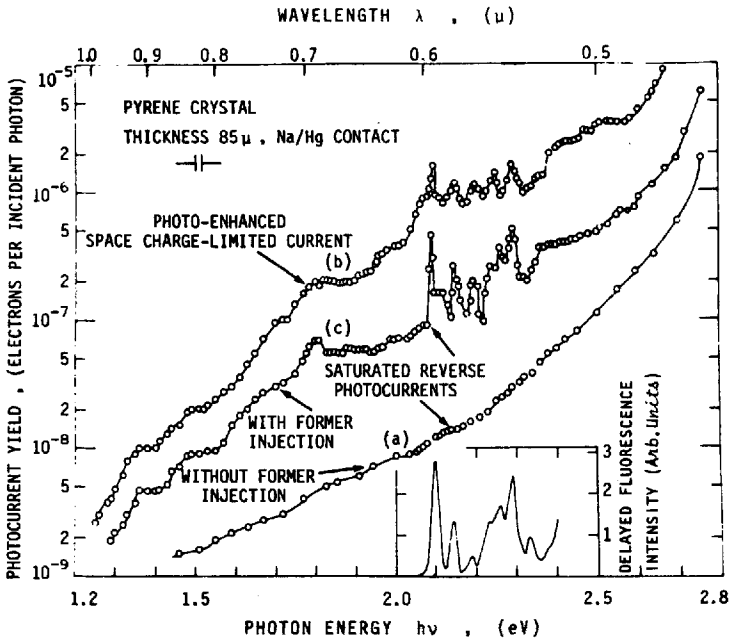

FIGURE 3 Spectral response of saturated reverse photocurrent yield. (a) without and (c) with former injection of electrons. The photo-enhanced space-charge-limited currents (b) is also shown. Insert is the excitation spectrum for delayed fluorescence after Avakian and Abramson (ref. 5).

injection with a forward voltage of 400 V. The light intensities used for taking this curve were sufficiently low such that several points (covering part of the spectrum) could be taken without appreciable bleaching. Re-filling of the traps by injection was necessary in order to cover the entire spectrum. On illuminating the crystal with white light, the photocurrents decay, and eventually the residual photocurrent spectrum of curve (a) is re-obtained.

Curves (b) and (c) are seen to be very similar, as expected. The latter, however, is more accurate since the dark currents present in the former introduce some noise.

Perhaps the most pronounced feature of curves (b) and (c) is the appearance of the triplet structure[5] in the range $2.05\ \text{eV} < h\nu < 2.4\ \text{eV}$. For comparison we inserted in the figure the excitation spectrum for delayed fluorescence in pyrene, as was measured by Avakian and Abramson.[5] The square root of this spectrum reflects the yield for excitation of triplet excitons[6] in pyrene. The case is therefore very similar to that of anthracene,[1] where in the triplet range, the photocurrent arises mainly from the interaction of photo-generated triplet excitons with trapped electrons.

At lower photon energies ($h\nu \lesssim 2.05$ eV), no triplet excitons are generated and de-trapping must occur by *direct* optical excitation. As will be shown below, the set of traps responsible for the photocurrents in this range is essentially discrete in energy so that the spectral yield reflects the structure at the conduction band in pyrene. One discerns clearly in curve (c) and to a somewhat lesser extent in curve (b)) four steps separated by (unequal) energy intervals of 0.1–0.2 eV. The fourth step starts at about 1.8 eV and is followed by a more or less constant yield with no structure, up to photon energy of about 2.05 eV. This indicates the presence in the lower part of the conduction band of three narrow sub-bands followed by a broader band. Such a structure is compatible with theoretical calculations[7] which suggest that the low-lying conduction states may consist of a series of narrow (0.01–0.1 eV) tight-binding conductivity bands separated by vibrational quanta of typically 0.1–0.2 eV. Somewhere above these tight-binding sub-bands one should expect a. broad, free-electron conduction band. The actual calculations were carried out for anthracene and naphtalene[7,8] but the similarity between the values of the electronic mobility in pyrene[4] and of anthracene and naphtalene[7] suggests that the situation in pyrene should not be very different. The vibronic splitting is reflected in the yield curves of Figure 3 in that the liberation of a trapped electron by an absorbed photon may involve the simultaneous excitation of one or more of the dominant vibrational modes in pyrene. The fact that the first three steps in the yield curves are well resolved indicates that the width of the tight-binding sub-band is smaller than the vibrational quanta involved (0.1–0.2 eV). At the same time, the absence of dips immediately after each step suggests a finite width in either

the tight-binding sub-band or the trap level. The rise in the first step provides an upper-limit estimate of about 0.1 eV for the combined width of the tight-binding band and the trap level. The situation is markedly different in that part of the yield curve representing the broad, free-electron conducting band (following the fourth step), where no structure is apparent. This is as expected since the excited electrons can be scattered by molecular vibrations within the broad band. The energy separation between the lowest-lying tight-binding sub-band and the bottom of the broad, free-electron band is seen to be about 0.45 eV. A lower-limit estimate for the width of the latter is 0.25 eV. The band is probably broader, extending beyond the point corresponding to a photon energy of 2.05 eV. In this range, however, de-trapping by triplet excitons becomes dominant and nothing much can be inferred from the yield spectrum as regards the band structure. In addition, as will be discussed below, a new set of traps becomes involved in the excitation process at photon energies above 2.05 eV.

The photocurrents in the high photon energy range ($h\nu > 2.4$ eV) may be due to direct de-trapping of electrons and/or to the interaction of photo-generated singlet excitons with the trapped electrons. These processes have not been studied in the present work. The origin of the residual photocurrents appearing in pyrene (curve (a)) have also not been studied. Since the triplet absorption spectrum is not reflected in this yield curve, the photocurrents at least in this photon-energy range must be due to direct optical excitation out of surface or bulk traps which are partly or completely occupied *under thermal equilibrium conditions*. For higher photon energies, interaction with photo-generated singlet excitons is also possible. Previous measurements on anthracene[9] showed that in that crystal the traps involved are mainly *surface* traps for *holes*.

We discuss next the trap distribution in the vapour-grown pyrene crystals studied. Curve (a) of Figure 4 represents the saturated reverse-photocurrent spectrum obtained immediately following injection, and is a reproduction of curve (c) in Figure 3. Curve (b) is the reverse-photocurrent spectrum obtained for the case in which injection is followed by prolonged illumination in the reverse polarity (bleaching) with light of photon energy of 1.80 eV ($\lambda = 0.69\ \mu$). Bleaching with light of photon energy of either 1.35 or 2.04 eV ($\lambda = 0.9\ \mu$ or $0.608\ \mu$) resulted in essentially the same curve. As a result of the bleaching the long-wavelength part of the spectrum is seen to disappear. (More precisely, the photocurrents are reduced to the value they had before injection—curve (a) of Figure 3.) The photocurrent starts to rise again at $h\nu > 2.05$ eV. Above this photon energy it maintains its former shape (the triplet structure) and the whole spectrum is reduced in magnitude by a factor of about 2–3. Since the threshold for detectable photocurrents is at about 1.3 eV, it follows that the spectrum in the range $1.3\text{ eV} < h\nu < 2.0\text{ eV}$

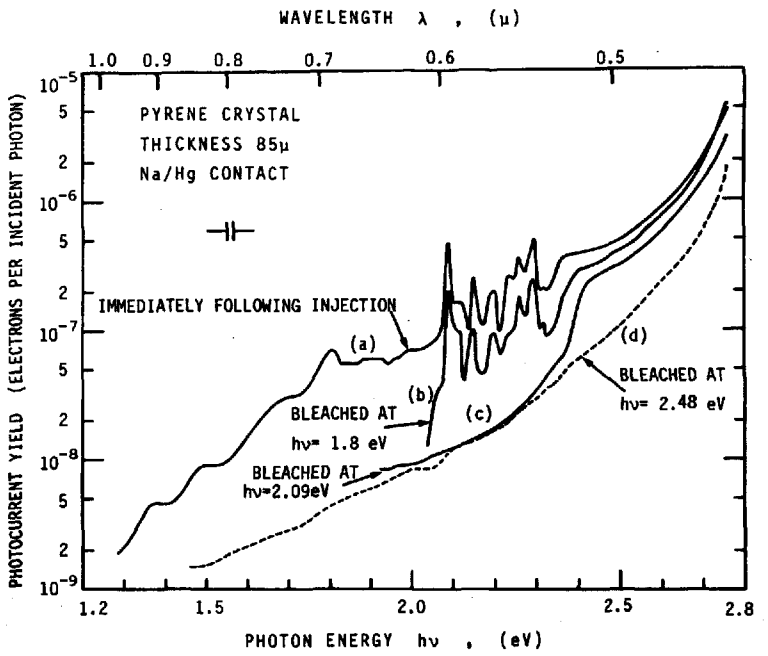

FIGURE 4 Spectral response of saturated reverse photocurrent yield. (a) immediately following injection, (b) after the shallow set of traps has been bleached out by prolonged illumination with $h\nu = 1.8$ eV, and (c) after the two shallower sets of traps have been bleached out by prolonged illumination with $h\nu = 2.09$ eV.

originates from photoexcitation of trapped electrons out of a single set of traps which is essentially discrete in energy and situated at about 1.35 eV below the lowest conduction sub-band. Moreover, since no triplet excitons are generated in this range, the optical excitation must be direct. The shoulder in curve (b) present at 2.05 eV indicates the onset of direct de-trapping of electrons from a second set of traps. That this set is also discrete in energy (width $\lesssim 0.05$ eV) is evidenced by curve (c). This curve has been obtained when injection is followed by bleaching of the crystal with light of photon energy of 2.09 eV (the first triplet peak). Here again bleaching with light of photon energy of 2.26 eV resulted in essentially the same curve. The photo de-trapping in the triplet range is due to two processes. A direct excitation, and excitation through the interaction of trapped electrons with photo-generated triplet excitons. The latter process can take place only through the lowest triplet state ($E = 2.09$ eV). Illumination at the first triplet peak will therefore result in the bleaching out of all the traps of lower energy which are available to interact with the triplet excitons. One therefore expects the triplet structure to disappear, as is really obtained and shown in curve (c).

However, unless the set of traps is shallower than 2.09 eV, one could expect to observe photocurrents due to the *direct* photoexcitation process in the range 2.1 eV $< h\nu <$ 2.3 eV. The absence of such photocurrents (no contribution above the value of the residual photocurrents) shows that the energy location of the second set must be within the range 2.05–2.09 eV.

The fast rise of the yield in curve (c) at about 2.35 eV indicates the existence of a third set of electron traps located at this energy range. The possibility for interaction with triplet excitons can be ruled out since, as mentioned above, this interaction can take place only through the lowest triplet state ($E = 2.09$ eV). The remaining possibilities are either direct photoexcitation or through the interaction of the trapped electrons with photo-generated singlet excitons. By illuminating the crystal with light of photon energy $h\nu = 2.48$ eV, the photocurrents in the whole range studied (1.2 eV $< h\nu <$ 2.8 eV) are bleached out, and the crystal returns to its virgin state (curve (d)). The width of this set is thus determined to be about 0.13 eV.

Estimates of the densities of traps responsible for the reverse photocurrents are provided by bleaching decay curves (reverse photocurrent vs. time of illumination). The saturated reverse photocurrent $J_s(t)$ is given by[1,2]

$$J_s(t) = (\tfrac{1}{2})qL(-\mathrm{d}n_t/\mathrm{d}t), \tag{1}$$

where n_t is the density of trapped electrons. We consider the case in which de-trapping can occur by both direct photoexcitation and by interaction with triplet excitons. For the sake of simplicity we first assume that only *one* set of traps is involved. In this case the rate of de-trapping can be expressed as

$$\mathrm{d}n_t/\mathrm{d}t = -(A_\lambda F n_t + R_t n_t T), \tag{2}$$

where T is the density of triplet excitons, R_t the rate constant characterizing the triplet exciton-trapped electron interaction, A_λ the cross-section for *direct* optical excitation and F is the photon flux density entering the sample. R_t can be expressed as $R_t = \sigma v_T$ where v_T is the triplet-exciton thermal velocity and σ is the cross section for de-trapping of electrons by the triplet excitons. For sufficiently low light intensities triplet-triplet annihilation can be neglected,[6] and the rate equation governing the triplet concentration is given by [6]

$$\mathrm{d}T/\mathrm{d}t = \alpha_\lambda F - T/\tau \tag{3}$$

Here α_λ is the triplet absorption coefficient and τ is the triplet lifetime in the sample. The influence of the triplet exciton–trapped electron interaction on the triplet lifetime is assumed to be negligible. ($R_t n_t < 1/\tau$). Steady-state conditions for the triplet concentration is obtained in a few triplet lifetimes

($\sim$5 msec) following the onset of illumination. For the light intensities used, this is considerably shorter than the decay-time of the reverse photocurrents (see Figures 5 and 6 below). Thus, the measured photocurrents correspond to steady-state conditions as far as the triplet concentration is concerned. The steady-state solution of Eq. (3) is

$$T = \alpha_\lambda F \tau \tag{4}$$

Inserting (4) into (2) and solving for Eq. (1) one obtains for the photocurrent density

$$\begin{aligned} J_s(t) &= J(0)\exp[-F(A_\lambda + R_t\alpha_\lambda\tau)t]; \\ J(0) &= (\tfrac{1}{2})qLn_t(0)F(A_\lambda + R_t\alpha_\lambda\tau), \end{aligned} \tag{5}$$

where $n_t(0)$ is the initial density of trapped electrons. When more than one set of traps is involved, $J_s(t)$ is given as a *sum* of such exponentials, each corresponding to one of the sets. Analysis of the decay curves of the reverse photocurrents can thus provide information on $n_t(0)$ as well as on the other parameters appearing in Eq. (5).

In Figure 5 the time decay of the saturated reverse photocurrent is plotted on a semi-log scale for illumination with light of photon energy of 1.8 eV (triangles) and of 2.04 eV (squares). For both cases only the shallow set of traps can participate. The traps are being emptied by direct optical excitation only since no triplet excitons are photo-generated in this range. As expected, the bleaching curves are both exponential (over more than an order of

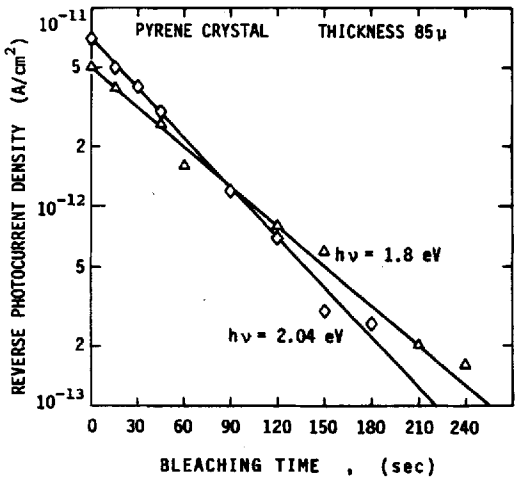

FIGURE 5 Semi-log plots of reverse photocurrent as function of bleaching time. Bleaching with $h\nu = 1.8$ eV, intensity $F = 10^{15}$ photons/cm^{2}sec (triangles) and with $h\nu = 2.04$ eV, intensity $F = 1.2 \times 10^{15}$ photons/cm^{2}sec (squares). Prior injecting voltage was 400 V.

magnitude in the photocurrent). The photon fluxes being almost identical ($\sim 10^{15}$ photons/cm^2 sec), the similarity in slope and magnitude of the two curves indicates that both indeed originate from the same set of traps. The common decay constant yields the product FA_λ whereas the initial photocurrent density $J(0)$ provides an estimate of $n_t(0)$ (see Eq. (5)). The values so determined are $A_\lambda \approx 1.5 \times 10^{-17}$ cm^2 and $n_t(0) \approx 5 \times 10^{11}$ cm^{-3}. Since the forward injecting voltage used was sufficiently large (400 V) to fill up all the traps of the set, the latter value represents the overall density of traps in this set.

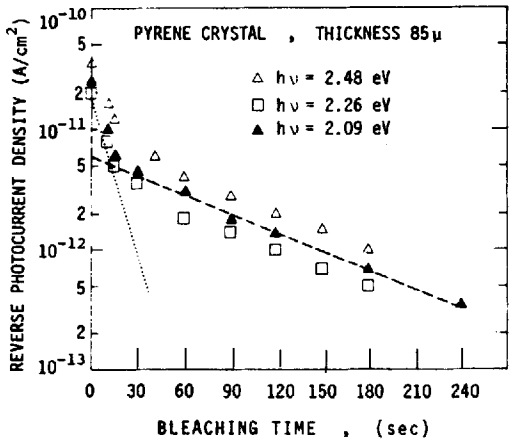

FIGURE 6 Semi-log plots of reverse photocurrent as function of bleaching time. Bleaching with $h\nu = 2.48$ eV, intensity $F = 6.5 \times 10^{14}$ photons/cm^{2}sec; $h\nu = 2.26$ eV with $F = 3.6 \times 10^{14}$ photons/cm^{2}sec; and $h\nu = 2.09$ eV (the first triplet peak) with $F = 3.8 \times 10^{14}$ photons/cm^{2}sec. Resolution of the bleaching curve for $h\nu = 2.09$ eV into two exponential components depicted by dashed straight lines.

Figure 6 presents bleaching curves obtained for illumination with light of photon energies 2.09 eV (full triangles), 2.26 eV (open squares) and 2.48 eV (open triangles). For $h\nu = 2.09$ eV and $h\nu = 2.26$ eV the two shallow sets are involved, and for $h\nu = 2.48$ eV excitation out of all three sets of traps takes place. This case is therefore more involved and indeed none of the curves is a pure exponential. Also, for $h\nu = 2.09$ eV and $h\nu = 2.26$ eV, the liberation of the trapped electrons takes place by both direct photoexcitation and by interaction with photo-generated triplet excitons. Nevertheless, the bleaching curves can be analized as will be illustrated for the case of illumination with $h\nu = 2.09$ eV. The two dashed straight lines in Figure 6 represent the resolution of the 2.09 eV bleaching curve into two exponentials corresponding to the two sets of traps (located at 1.35 eV and 2.08 eV below the lowest conduction band). The densities of traps for the fast and slow

components can be estimated as in the case of Figure 5 and are found to be $n_{t1}(0) \approx 3 \times 10^{11}$ cm^{-3} and $n_{t2}(0) \approx 6 \times 10^{11}$ cm^{-3} respectively. If now the crystal is illuminated with light of any photon energy in the range 1.3 eV < $h\nu$ < 2.04 eV, the fast component is bleached out while the slow component remains unchanged. This indicates clearly that the shallow set is responsible for the fast component, while the slow component arises from de-trapping out of the *second* set of traps.

The characteristic parameters of the three sets of traps, as derived from an analysis of the bleaching curves of Figures 5 and 6, are listed in Table I. The analysis is based on Eq. (5) on the one hand and on a number of parameters associated with the triplet excitons on the other. The triplet lifetime as determined by the phase-shift method[10] was 1.2 msec. For the triplet thermal velocity we took the value of[11] $v_T = 8 \times 10^3$ cm/sec while the triplet absorption coefficient was taken as[12] $\alpha_\lambda \approx 10^{-3}$ cm^{-1} at the first triplet peak.

TABLE I

Summary of the various parameters characterizing the three sets of traps present in the pyrene crystal under study

	First set	Second set	Third set
depth (eV)	~1.35	2.05–2.09	2.35–2.48
density (cm^{-3})	$\sim 5 \times 10^{11}$	$\sim 5 \times 10^{11}$	$\sim 5 \times 10^{11}$
A_λ (cm^2)	$\sim 1.5 \times 10^{-17}$ for $h\nu = 1.8$ eV and 2.04 eV $\sim 5 \times 10^{-17}$ for $h\nu = 2.09$ eV	$\sim 5 \times 10^{-18}$ for $h\nu = 2.09$ eV	
R_t (cm^3/sec)	$\sim 2 \times 10^{-10}$	$\sim 2 \times 10^{-11}$	
σ (cm^2)	$\sim 2 \times 10^{-15}$	$\sim 2 \times 10^{-16}$	

We also assumed that the variation in the yield for direct optical de-trapping is not large in the range of the first triplet peak. On this assumption the contribution of the triplets to the overall excitation yield could be obtained by subtracting the yield just below the peak from that at the peak.

There is not much point in carrying out a similar analysis for the bleaching curve at $h\nu = 2.48$ eV (triangles in Figure 6) since the nature of the de-trapping process is not clear. From the area under the curve, however, one obtains a rough estimate of $\sim 10^{12}$ cm^{-3} for the density of all the three sets of traps involved. This value is about one order of magnitude smaller than the density estimated on the basis of the trap-filled limit V_{TFL}. It appears therefore that most of the traps controlling V_{TFL} are shallow so that they are thermally bleached before a reverse photocurrent measurement is taken (5–10 minutes after injection).

CONCLUSION

The spectral yield of the photocurrent arising from the photoexcitation of trapped electrons points to the existence in pyrene of a series of narrow ($\lesssim$0.1 eV) conducting sub-bands which constitute the bottom of the conduction band. The energy separation between adjacent sub-bands varies between 0.1 and 0.2 eV, as expected for splittings of a narrow band by molecular vibrations.[8] The results indicate also the presence of a broad, free-electron band, at least 0.25 eV in width, the bottom of which lying about 0.45 eV above the lowest conducting sub-band. In contrast to the case of anthracene,[1] the two types of conducting states are well resolved experimentally.

The derivation of these characteristics of the conduction-band structure in pyrene was made possible by the fact that only one discrete set of traps contributes to the spectral yield of the photocurrent in the range of interest. This set is located 1.3 eV below the lowest conduction sub-band and is of density of about 5×10^{11} cm^{-3}. Two other sets of traps of comparable density, located at 2.07 and 2.4 eV below the lowest sub-band, were also identified. The data provided a fairly detailed characterization of these traps (see Table I).

In the range 2.05 eV $< h\nu <$ 2.4 eV the spectral yield curve reflects very clearly the triplet-exciton excitation structure. Here de-trapping is mainly due to the interaction of trapped electrons with photo-generated triplet excitons. The interaction rates for the first two sets of traps were determined (Table I).

The nature and origin of the traps in the vapour-grown samples studied in not known. The primary objective of this investigation has been to utilize the traps as a means of studying the conduction-band structure. For this purpose all that is required is to establish that they have the necessary characteristic, namely, suitable location and discreteness in energy.

Acknowledgements

The authors are indebted to Professor A. Many for stimulating discussions and critical reading of the manuscript.

References

1. A. Many, J. Levinson, and I. Teucher, *Molecular Crystals*, **5**, 273 (1968).
2. Z. Burshtein and A. Many, *Mol. Cryst. Liq. Cryst.*, **25**, 31 (1974).
3. M. A. Lampert, Reports on Progress in Physics, **27**, 329 (1964).
4. W. Bepler, *Z. Physik*, **185**, 507 (1965).

5. P. Avakian and E. Abramson, *J. Chem. Phys.*, **43**, (3), 821 (1965).
6. P. Avakian and R. E. Merrifield, *Molecular Crystals*, **5**, 37 (1968).
7. O. H. LeBlanc, Jr., in *Physics and Chemistry of the Organic Solid State*, Vol. III, D. Fox, M. M. Labes, and A. Weissberger, Editors (Interscience Publishers 1967), p. 133, and references cited therein.
8. R. Silbey, J. Jortner, S. A. Rice, and M. T. Vala, *J. Chem. Phys.*, **42**, 733 (1965) and Erratum **43**, 2925 (1965).
9. J. Levinson, Z. Burshtein, and A. Many, *Mol. Cryst. Liq. Cryst.*, **26**, 329 (1974).
10. V. Ern, *Phys. Rev. Lett.*, **22**, 343 (1969).
11. S. Arnold, W. B. Whitten, and A. C. Damask, *Phys. Rev.*, **B3**, 10, 3452 (1971).
12. H. Bouchriha, M. Schott, M. Bisceglia, and G. Delacote, *Chem. Phys. Lett.*, **23**, (2), 183 (1973).